Monatshefte für Chemie 133, 285–298 (2002)

Monatshefte für Chemie
Chemical Monthly

Electronic Structure of Cu(II) Complexes with N,N′-Disalicylidene-1,2-cyclohexanediamine and N,N′-Disalicylidenetrimethylenediamine

Miki Hasegawa[1,*], **Ken-ichi Kumagai**[1], **Mayumi Terauchi**[1], **Akiko Nakao**[2], **Jun Okubo**[3], and **Toshihiko Hoshi**[1]

[1] Department of Chemistry, College of Science and Engineering, Aoyama Gakuin University, Tokyo 157-8572, Japan
[2] Mac Science Co. Ltd., Yokohama, Kanagawa 222-0033, Japan
[3] Department of Natural Science for General Education, Faculty of Engineering, Tokyo Denki University, Chiba 270-1382, Japan

Summary. The electronic absorption and X-ray photoelectron spectra of N,N′-disalicylidenetrimethylenediaminatocopper(II) ([Cu(*saltn*)]) and N,N′-disalicylidene-*trans*-1,2-cyclohexanediaminatocopper(II) ([Cu(*salchx*)]) were measured. From these results and from informations derived from MO calculations the electronic structure of the complexes was clarified. Each electronic absorption band which can be assigned to the $\pi\pi^*$ or *ML*/*LM*CT transition of [Cu(*saltn*)] or [Cu(*salchx*)] observed in the wavelength region of 450–200 nm appears at the almost same frequency as the corresponding band of N,N′-disalicylideneethylenediaminatocopper(II) ([Cu(*salen*)]) in solution. The *LL*CT bands (the intramolecular CT band between two π-electronic systems separated by saturated hydrocarbon chains such as $-(CH_2)_{n}-$) also appear at nearly the same positions (*ca.* 245 nm) for [Cu(*salchx*)], [Cu(*saltn*)], and [Cu(*salen*)]. The locations of the dd transition and the intensity of the *ML*/*LM*CT transition of [Cu(*saltn*)] are significantly different from those of [Cu(*salen*)] and [Cu(*salchx*)]. These differences may arise from the strengths of the interaction between metal and ligand.

Keywords. Electronic absorption spectra; *Schiff* base complexes; X-Ray photoelectron spectroscopy; Electronic structure.

Introduction

N,N′-Disalicylideneethylenediamine (*salen*), one of the typical bridged *Schiff* bases, easily forms complexes with metal ions such as copper(II) or nickel(II). Synthetic and spectroscopic studies on the metal complexes with *Schiff* bases have been performed by many investigators [1–12]. Recently, some *Schiff* base metal complexes have been utilized as catalysts in the selective syntheses of enantiomers or as probes for *DNA* [13–21]. For instance, a manganese(III) complex with a derivative of *salen* has been used as a catalyst to cleave *DNA* photochemically

* Corresponding author. E-mail: hasemiki@chem.aoyama.ac.jp

selectively at the T-site [18]. Analogues of salen like N,N′-disalicylidenetrimethylenediamine (*saltn*) or N,N′-disalicylidene-*trans*-1,2-cyclohexanediamine (*salchx*) also easily form complexes with metal ions. X-Ray analyses of [Cu(*salen*)], [Cu(*saltn*)], and [Cu(*salchx*)] have already been performed [11, 12, 22–24]. The copper(II) in [Cu(*salen*)] adopts a square planar structure, *i.e.* the two salicylideneimino group planes are almost coplanar [11, 12]. On the other hand, the two salicylideneimino group planes are not coplanar in [Cu(*saltn*)] and [Cu(*salchx*)]; the dihedral angle between the two planes amounts to about 40° in [Cu(*saltn*)] and 20° in [Cu(*salchx*)] [22–24]. [Cu(*salen*)] forms dimers in the crystalline state through two Cu $\cdots$ O bonds [11, 12]. This kind of dimerization also occurs in a 5:5:2 solvent mixture of diethyl ether, 2-methylbutane, and ethanol at low temperature [1]. Every copper(II) complex mentioned above has two almost independent π systems (π and π') localized on the two salicylideneimino groups. As for [Cu(*salen*)], the electronic structure has been elucidated from the viewpoints of polarization spectra and extended PPP MO calculations [1]. [Cu(*salen*)] shows longer molecular axis polarized bands at $382(\pi\pi_1^*)$, $\sim 290(\pi\pi_3^*)$, $\sim 250(\pi\pi_6^*)$, and $230.4(\pi\pi_7^*)$ nm and shorter molecular axis bands at $354(\pi\pi_2^*)$, $273.0(\pi\pi_4^*)$, 242.4, and $\sim 220(\pi\pi_8^*)$ nm; the 242.4 nm band is assigned to an intramolecular CT transition between the metal ion and the ligand. Furthermore, a band assigned to a dd transition is observed at 565 nm in ethanol. Several papers concerning the electronic transitions of nickel(II), calcium(II), or copper(II) complexes with *saltn* or *salchx* have been reported [24–26]. For instance, [Ni(*saltn*)] shows absorption bands at 588 nm in chloroform and at 614 and 560 nm in pyridine, from which it is estimated that the nickel(II) complex is square planar in chloroform and octahedral in pyridine. The diffuse reflection spectrum of [Ni(*saltn*)] recrystallized from pyridine well reproduces the absorption spectrum measured in pyridine. However, there are no detailed descriptions on the nature of electronic transitions except for the dd transitions. In this investigation, measurements of electronic absorption and X-ray photoelectron spectra as well as MO calculations have been performed for [Cu(*saltn*)] and [Cu(*salchx*)] from which the electronic structures of the metal complexes are discussed. Moreover, the mechanisms of the interactions between two π systems existing almost independently in the complexes have been elucidated. It is very difficult to realize the origins of electronic transitions without the aid of MO calculations. During the past three or four decades, many kinds of MO approximations have been proposed; however, MO approximations reproducing electronic absorption spectra of metal complexes with organic ligands are not available. For instance, the ZINDO method by *Zerner et al.* can reproduce well electronic absorption spectra of ordinary organic compounds [27, 28]. However, it may be not useful to employ the ZINDO method for the interpretation of electronic spectra of metal complexes with organic ligands. In fact, we performed ZINDO calculations on [Cu(*saltn*)], but dd transition energies were obtained which were too high compared with the observed ones, and *LM*CT transition energies were too low [29]. Thus, a point charge approximation was adopted to interpret the electronic transitions of the metal complex treated here. As for [Cu(*saltn*)], a single crystal X-ray structural analysis has already been performed [22, 23], but the described molecular packing does not seem to be correct. Therefore, the X-ray structural analysis was repeated.

Results and Discussion

Electronic absorption spectra

Figure 1 shows the electronic absorption spectra of [Cu(*saltn*)] and [Cu(*salchx*)] in ethanol; the spectrum of [Cu(*salen*)] is also shown for comparison. The absorption bands in the wavelength region of 450–200 nm of the three complexes are very similar. This indicates that the complexes have similar π electronic structures. The dd transitions of [Cu(*salen*)] and [Cu(*salchx*)] appear at almost identical positions (565 and 560 nm, respectively), whereas that of [Cu(*saltn*)], in which the two salicylideneimino planes are heavily twisted, is red-shifted by about 40 nm.

Figure 2 shows the solid state absorption spectra of [Cu(*salen*)], [Cu(*salchx*)], and [Cu(*saltn*)] in KBr disks. The locations and relative intensities of the bands of [Cu(*salen*)] and [Cu(*saltn*)] well reproduce those observed in solutions. This indicates that the intermolecular interactions of [Cu(*salen*)] and [Cu(*saltn*)] are not large even in the solid state. However, the solid state spectrum of [Cu(*salchx*)] is broader compared with that observed in solution, and its relative intensities differ from those in solution. That is, in the case of [Cu(*salchx*)] intermolecular interactions are considerably large in contrast to [Cu(*salen*)] and [Cu(*saltn*)].

In order to gain information on a more detailed electronic nature of [Cu(*saltn*)] and [Cu(*salchx*)], the polarized absorption spectra in stretched *PVA* films have been measured; the results are shown in Figs. 3 and 4, respectively. For [Cu(*saltn*)], the 362 and 243 nm bands with minima in the *Rd* curve are polarized along the shorter molecular axis, and the 300 (shoulder) and 230.0 nm bands with maxima along the longer molecular axis (Fig. 3). The *Rd* values increase at the longer wavelength side of the 362 nm band, indicating that an additional longer molecular axis polarized band is hidden at this location (around 400 nm). Similarly, it can be seen

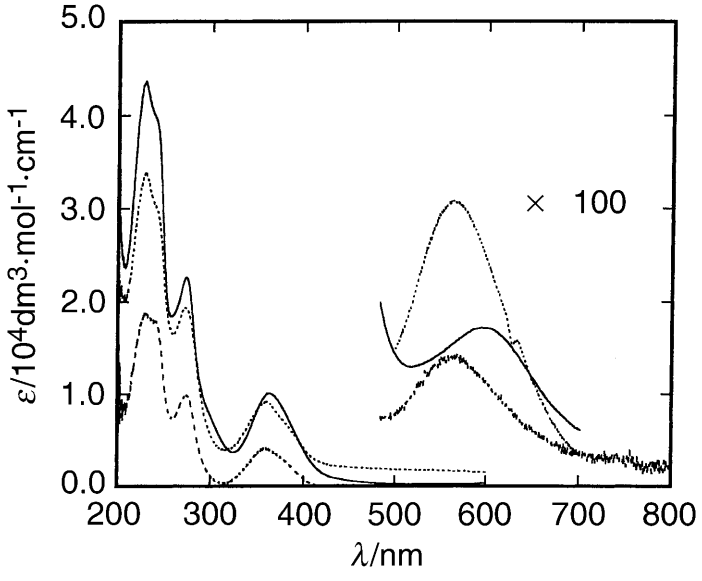

Fig. 1. Electronic absorption spectra of [Cu(*saltn*)] (solid line), [Cu(*salchx*)] (dotted line), and [Cu(*salen*)] (dashed line) in ethanol

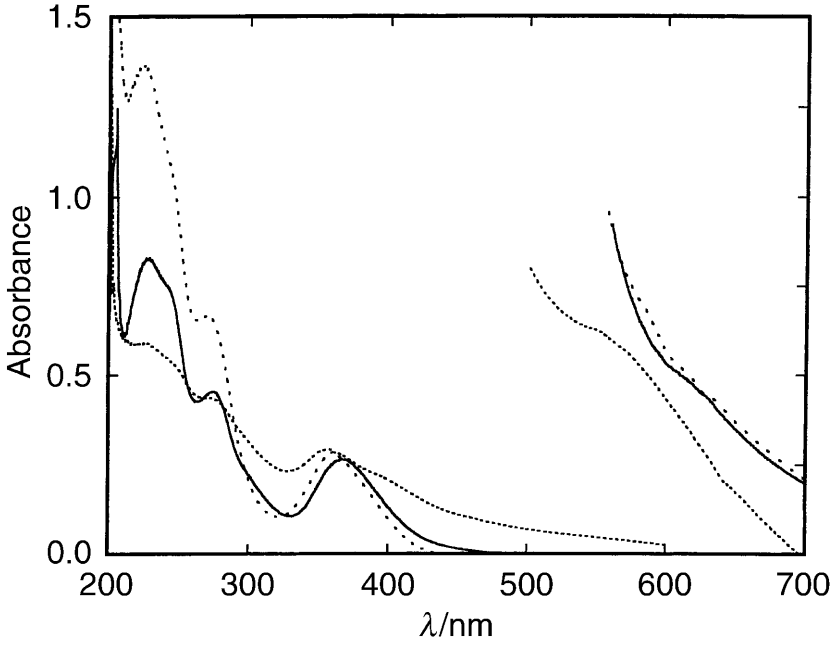

Fig. 2. Solid state electronic absorption spectra of [Cu(*saltn*)] (solid line), [Cu(*salchx*)] (dotted line), and [Cu(*salen*)] (dashed line) in KBr disks

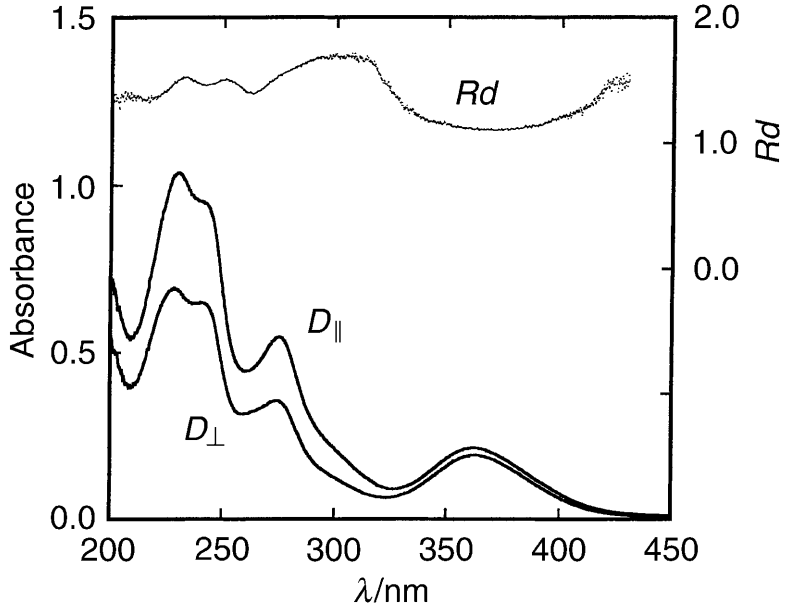

Fig. 3. Polarized absorption spectrum of [Cu(*saltn*)] in a stretched *PVA* film; $D_{\parallel}$, $D_{\perp}$: optical densities measured with light polarized parallel and perpendicular to the stretching direction; $Rd = D_{\parallel}/D_{\perp}$

that shorter (or intermediate) molecular axis polarized bands are hidden at around 262 and 220 nm. Moreover, an additional longer molecular axis polarized band is expected at around 250 nm, because a maximum is found in the *Rd* curve at this

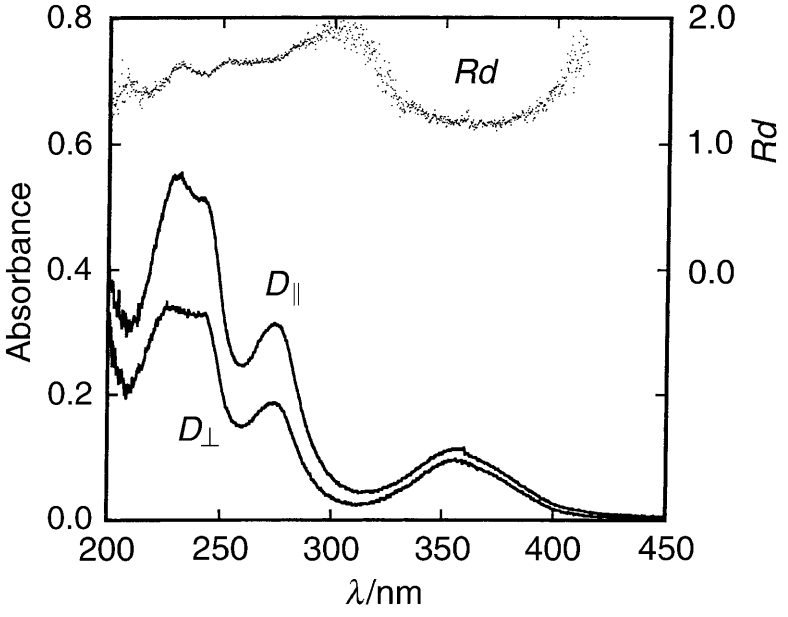

Fig. 4. Polarized absorption spectrum of [Cu(*salchx*)] in a stretched *PVA* film; $D_{\parallel}$, $D_{\perp}$, *Rd*: see Fig. 3

position. In the wavelength region of 320–260 nm, the *Rd* values decrease with a decreasing wavelength, indicating that two differently polarized bands exist in this wavelength region, *i.e.* the 300 nm band is polarized along the longer molecular axis, and the 276.3 nm band along the shorter one.

In the case of [Cu(*salchx*)] it is obvious that the 358 and 242 nm bands with minima in the *Rd* curve are polarized along the shorter molecular axis and the 231.3 nm band with a maximum along the longer molecular axis (Fig. 4). Longer molecular axis polarized bands are hidden at about 400 and 300 nm, because the *Rd* values increase clearly towards the longer wavelength side of 400 nm and approach a maximum at around 300 nm. The corresponding band to the former is recognized in the spectrum in alcohol as a weak shoulder at *ca*. 384 nm. Since the approximate symmetry of [Cu(*salchx*)] is C_{2v}, the broad 276 nm band is polarized along the shorter or longer molecular axis. As the corresponding calculated polarization is along the shorter molecular axis, the observed 276 nm band is considered to be polarized along the shorter molecular axis. In addition to the above bands, two bands are recognized at 250 (longer axis polarized) and 220 (shorter or intermediate molecular axis polarized) nm, since the *Rd* curve shows a maximum at 250 nm and a minimum at 220 nm.

Single crystal X-ray diffraction analysis

As described in the previous section, the absorption spectrum of the solid state [Cu(*saltn*)] is very similar to that observed in solution, *i.e.* even in the solid state [Cu(*saltn*)] does not show any additional bands originating from intermolecular interactions. Thus, it may be very interesting to know the molecular structure and the packing of [Cu(*saltn*)] in the crystalline state (Fig. 5). In [Cu(*saltn*)], Cu(II)

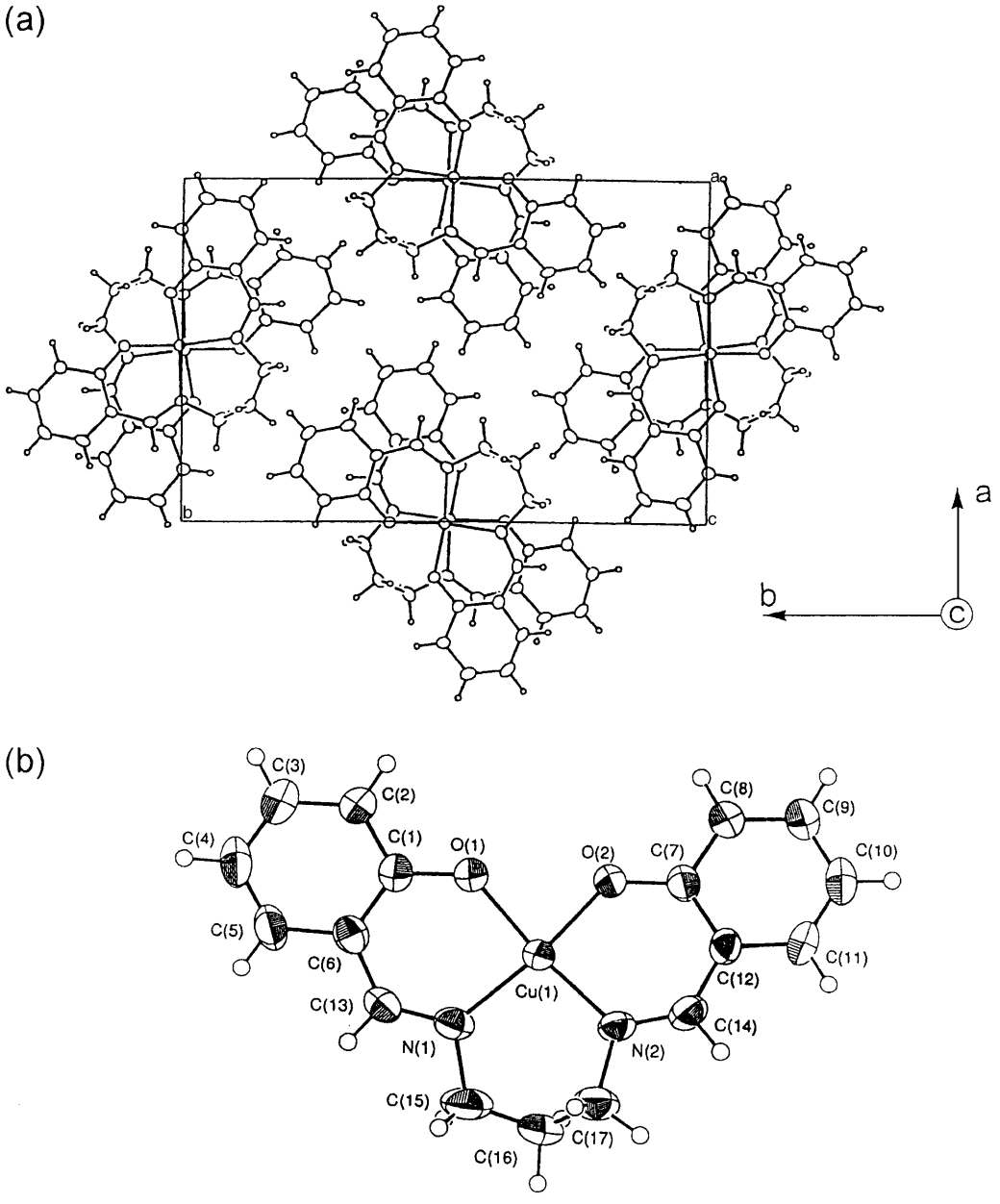

Fig. 5. (a) Molecular packing projected along the *c*-axis; (b) ORTEP drawing of [Cu(*saltn*)]

adopts a strongly distorted tetrahedral arrangement, and the two salicylideneimino group planes are twisted by about 40°. [Cu(*saltn*)] forms a column structure along the *c*-axis in which the two neighbouring molecules are arranged oppositely and the π systems of the two molecules are almost not overlapped. For instance, the nearest neighbour intermolecular–interatomic distance is 3.294 Å (C(6)–C′(14)), but the overlap of the two π orbitals seems to be very small owing to the twist of the C(6) and C′(14) π orbitals. These results of the X-ray structural analysis support the results obtained from the electronic absorption spectra in the solid state.

Table 1. Cu 2p XPS bands of [Cu(*salen*)], [Cu(*salchx*)], and [Cu(*saltn*)]

	Cu $2p_{3/2}$ (shake-up bands)/eV	Cu $2p_{1/2}$ (shake-up bands)/eV
[Cu(*saltn*)]	933.2 (938, 943)	953.2 (957, 962)
[Cu(*salchx*)]	932.9 (937, 943)	953.0 (958, 962)
[Cu(*salen*)]	932.6 (937, 943)	952.4 (957, 961)

X-Ray photoelectron spectroscopy

The XPS of [Cu(*saltn*)], [Cu(*salchx*)], and [Cu(*salen*)] were measured to gain a more detailed insight in the electronic structure of the central atom. Table 1 shows the Cu 2p binding energies of the three complexes which are known to decrease with increasing degree of interactions between Cu(II) and the ligand [30]. The Cu 2p band of [Cu(*salchx*)] is observed at higher energy compared with that of [Cu(*salen*)], meaning that Cu(II) less strongly interacts with *salchx* than with *salen*. Similarly, the Cu 2p band of [Cu(*saltn*)] is observed at higher energy than that of [Cu(*salchx*)]. These results clearly indicate that the degree of interaction between metal ion and ligands decreases with an increase in the twist angle of the π systems of the two salicylideneimino moieties.

Assignment of electronic absorption bands

Generally, Cu(II) or Ni(II) complexes with organic ligands show $\pi\pi^*$ electronic absorption bands of the ligands at higher energy and dd band based on the central metal ions at lower energy. For instance, *bis*-(tropolonato)-Cu(II) (*tro*Cu(II)) shows $\pi\pi^*$ bands of the ligand at 387 and 338 nm [31] which correspond to the 400 and 336 nm bands of the ligand itself [32]. *Bis*-(tropolonato)-Ni(II) (*tro*Ni(II)) also shows the corresponding bands at 402 and 339 nm [33]. *tro*Cu(II) and *tro*Ni(II) have different spin states. However, the bands of the two complexes originating from the ligands are corresponding well to each other, meaning that the interactions between the π and d electronic systems are negligibly small. Therefore, as a first approximation, the wavefunctions for the π and d electronic systems of the metal complexes can be virtually treated separately. That is, the d electronic systems can be treated as systems perturbed by the ligand field, and the π electronic systems localized on the ligands as systems perturbed by the central metal ion field.

As for the electronic structure and the nature of electronic transitions of [Cu(*salen*)], detailed analyses have already been performed [1]. In this section, the electronic spectra of [Cu(*salchx*)] and [Cu(*saltn*)] are discussed in comparison with that of [Cu(*salen*)]. As described in the previous section, [Cu(*saltn*)] has almost the same structure both in the solid and the solution state. Thus, the geometry obtained from the X-ray structural analysis was used for MO calculations. [Cu(*salchx*)] shows very broad electronic bands in the solid state, different from the band shapes in solution. This means that the structures of [Cu(*salchx*)] in solution and in the solid state are significantly different from each other, but each band in the solid state corresponds well to that measured in solution. Table 2 shows the results calculated for [Cu(*saltn*)] compared with the experimental data. The calculated transition energies, relative intensities, and polarization directions reproduce well

Table 2. Calculated and observed results for the electronic transitions of [Cu(*saltn*)]

	Transition energy/nm			Intensity		Polarization direction		
	calcd.	obsd.[a]		calcd.[b]	obsd.[c]	calcd.[d]		obsd.
						θ	ϕ	
			(600)[e]		(170)[f]			(dd*)
$\pi\pi_1^*$	332.5	~400	(384)	0.02395	shoulder	13.68	38.48	L
$\pi\pi_2^*$	327.1	362	(361.4)	0.18853	0.194 (9840)	52.42	91.82	S
$\pi\pi_3^*$	280.9	300	(300)	0.20247	0.209 (7570)	−40.34	106.34	L
$\pi\pi_4^*$	272.9	276.3	(274.2)	0.37974	0.532 (23240)	49.88	89.21	S
$\pi\pi_5^*$	239.9	262	(268)	0.00268	shoulder	−41.38	94.83	S or I
$\pi\pi_6^*$	239.8	250		0.00243	shoulder	−36.62	84.79	L
		243[g]	(243)		shoulder			S
$\pi\pi_7^*$	233.9	230.0	(228.8)	1.05278	1.000 (44590)	−39.33	92.01	L
$\pi\pi_8^*$	229.7			0.03090		−33.63	101.35	
$\pi\pi_9^*$	224.3	220		0.39247	shoulder	−40.55	102.36	S or I
$\pi\pi_{10}^*$	219.2			0.53911		49.98	91.01	

[a] Observed in the stretched *PVA* film; [b] oscillator strength; [c] observed relative intensity with respect to the 230.0 nm band; [d] see figure below; [e] observed in ethanol; [f] absorbance coefficient in ethanol; [g] CT transition between metal ion and ligand; S: shorter molecular axis; L: longer molecular axis; I: intermediate direction between shorter and longer axes

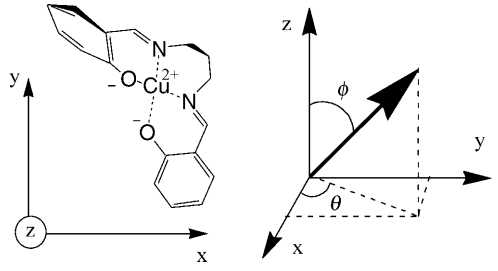

the observed results for [Cu(*saltn*)]. Furthermore, two allowed transitions ($\pi\pi_9^*$ and $\pi\pi_{10}^*$) are computed being assigned to the observed band at around 220 nm as a shoulder. The observed 243 nm band may be assigned as an intramolecular CT transition between the ligand and the metal ion (*ML*/*LM*CT), since the transition energy corresponding to the observed band is not found in the MO calculation.

The following equations show the excited state wavefunctions for [Cu(*saltn*)]:

$$\Psi_1 = -0.7075\chi_{10,11} + 0.5731\chi_{9,12} + \cdots$$
$$\Psi_2 = 0.5275\chi_{10,12} - 0.5196\chi_{9,11} - 0.4314\chi_{9,12} + \cdots$$
$$\Psi_3 = 0.5489\chi_{8,11} - 0.5320\chi_{7,12} + \cdots$$
$$\Psi_4 = -0.5456\chi_{8,12} - 0.5404\chi_{7,11} + 0.2360\chi_{10,13} + \cdots$$

Here, $\chi_{i,j}$ means a configuration wavefunction corresponding to the one-electron excitation from the i^{th} occupied MO to the j^{th} unoccupied one. The MOs used for the above excited state wavefunctions of [Cu(*saltn*)] are diagrammatically

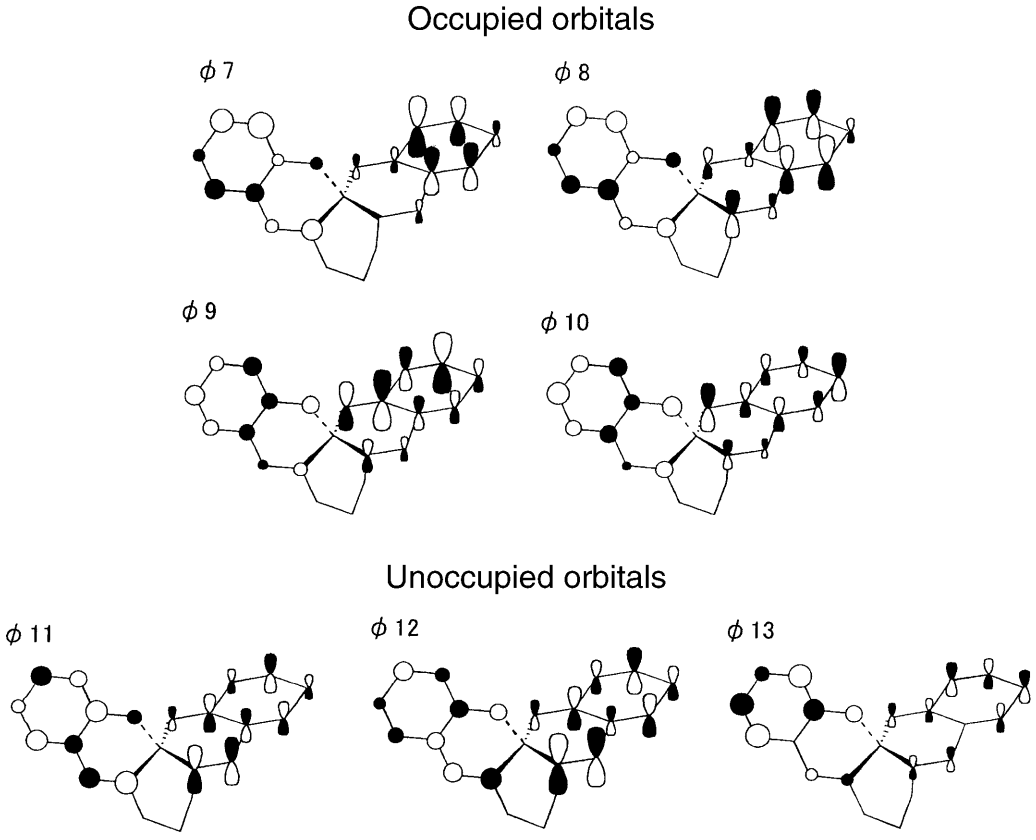

Fig. 6. Diagrammatic representations of MOs for [Cu(*saltn*)]

shown in Fig. 6. The main contributors to Ψ_1 corresponding to the $\pi\pi_1^*$ transition are $\chi_{10,11}$ and $\chi_{9,12}$. Thus, LUMO $\leftarrow$ HOMO and (LUMO + 1) $\leftarrow$ (HOMO − 1) transitions contribute by 50 and 33%, respectively, to the $\pi\pi_1^*$ transition. Similarly, the main contributors to the $\pi\pi_2^*$ transition are $\chi_{10,12}$ (28%), $\chi_{9,12}$ (19%), and $\chi_{9,11}$ (27%), and the observed 362 nm band can be interpreted as an intramolecular CT transition from the benzene moiety to the azomethine residue. Both $\pi\pi_3^*$ and $\pi\pi_4^*$ are considered to be a superposition of two intramolecular CT transitions from the benzene ring to the oxide and the azomethine groups.

In order to know a more detailed nature of the electronic transitions, configuration analysis (CA) has been performed on [Cu(*saltn*)] (Fig. 7) [34]. In the CA calculation, the structure in which two salicylideneimino moieties are separated infinitely is used for a reference molecule. It is seen that Ψ_1^0 contributes to both Ψ_1 and Ψ_2 by about 90%, and Ψ_2^0 also contributes to both Ψ_3 and Ψ_4 by about 90%. Here, Ψ_i^0 means the i^{th} excited state wavefunction of the reference molecule. Thus, the $\pi\pi_1^*$ and $\pi\pi_2^*$ transitions of [Cu(*saltn*)] are regarded as the first transition of the ligand, and the $\pi\pi_3^*$ and $\pi\pi_4^*$ transitions as the second transition of the ligand. Ψ_5, Ψ_6, Ψ_{11}, and Ψ_{12} correspond to the intramolecular CT (*LL*CT) transitions between the two π electronic systems existing almost independently.

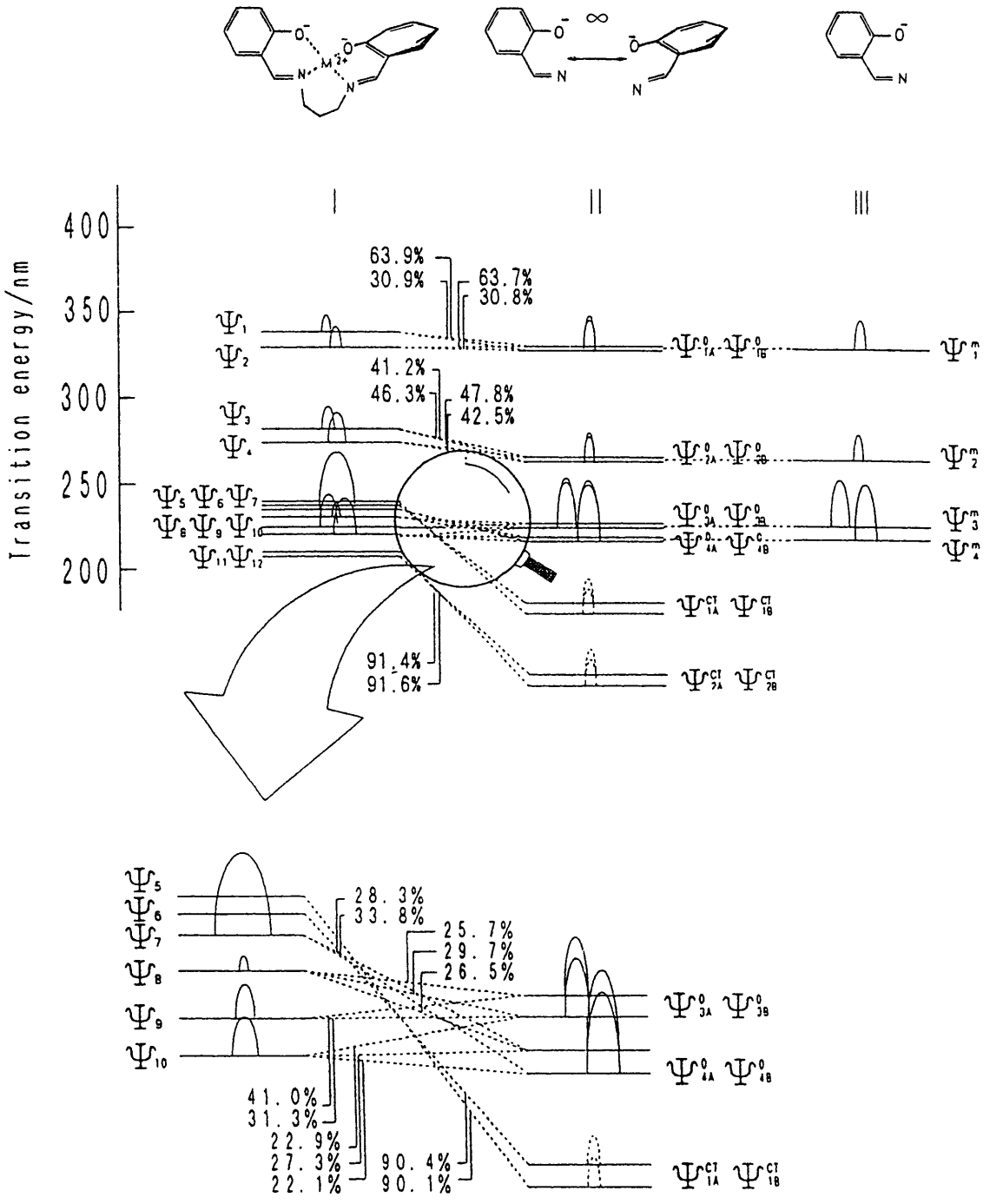

Fig. 7. Correlation diagram obtained from configuration analysis; I: energies of the n^{th} excited states (Ψ_n) with respect to the ground states (Ψ_G) for [Cu(*saltn*)]; II: energies of the n^{th} excited states ($\Psi^0_{n\text{A}}$ and $\Psi^0_{n\text{B}}$) of the reference molecule; III: energies of the n^{th} excited state (Ψ^m_n) of the salicylideneimine anion

Table 3. Calculated and observed results for the electronic transitions of [Cu(*salchx*)]

	Transition energy/nm			Intensity		Polarization direction		
	calcd.	obsd.[a]		calcd.[b]	obsd.[c]	calcd.[d]		obsd.
						θ	ϕ	
			(560)[e]		(130)[f]			(dd*)
$\pi\pi_1^*$	340.6	~400	(384)	0.00839	shoulder	0.00	177.25	L
$\pi\pi_2^*$	355.8	358	(358.1)	0.22144	0.203 (3480)	90.00	90.00	S
$\pi\pi_3^*$	283.3	300	(290)	0.25651	shoulder	0.00	99.75	L
$\pi\pi_4^*$	276.9	276	(274.2)	0.24561	0.582 (9840)	90.00	90.00	S
$\pi\pi_5^*$	237.6	260		0.02599	shoulder	90.00	90.00	S or I
$\pi\pi_6^*$	237.6	250		0.00163	shoulder	0.00	88.07	L
		242[g]	(242)		shoulder			S
$\pi\pi_7^*$	236.2	231.3	(229.0)	0.77600	1.000 (18770)	0.00	88.28	L
$\pi\pi_9^*$	225.4			0.67805		0.00	97.05	
$\pi\pi_8^*$	233.7			0.00047		90.00	90.00	
$\pi\pi_{10}^*$	220.5	220	(220)	0.40140	shoulder	90.00	90.00	S or I

[a] Observed in the stretched *PVA* film; [b] oscillator strength; [c] observed relative intensity with respect to the 231.3 nm band; [d] see figure below; [e] observed in ethanol; [f] absorbance coefficient in ethanol; [g] CT transition between metal ion and ligand; S: shorter molecular axis; L: longer molecular axis; I: intermediate direction between the shorter and longer axes

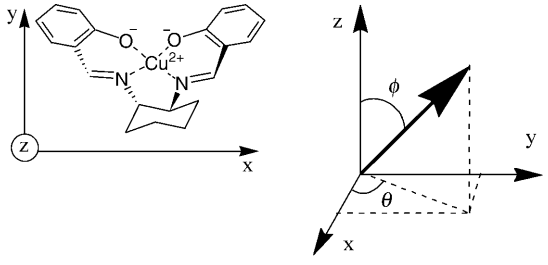

As described above, the structure of [Cu(*salchx*)] in solution is considered to be different from that in the solid state, but as a first approximation we performed an MO calculation for [Cu(*salchx*)] using the molecular geometry obtained from the X-ray structural analysis; the results are shown in Table 3. The calculated results well explain the observations except for the polarization direction of the first $\pi\pi^*$ transition. That is, the calculated $\pi\pi_1^*$ transition is computed to be polarized out of plane, the shorter molecular axis, but the corresponding observed band with large *Rd* values (Fig. 4) is polarized along the longer molecular axis. The shapes of the polarized absorption spectrum and the *Rd* curve are similar to those of [Cu(*salen*)] rather than to those of [Cu(*saltn*)] [1]. This indicates that [Cu(*salchx*)] adopts an approximately planar structure in solution. These results are also supported by the fact that the dd bands of [Cu(*salchx*)] and [Cu(*salen*)] are very similar to each other in shape and appear at almost the same frequencies. According to CA calculations, $\pi\pi_5^*$ and $\pi\pi_6^*$ transitions are regarded as *LL*CT transitions. The 242 nm band is due to an *ML*/*LM*CT transition similar to the 243 nm band of [Cu(*saltn*)].

Experimental

Materials

[Cu(*saltn*)] [35, 36]: 4 g of *bis*-(salicylidene)-copper(II) ([Cu(*sal*)$_2$], [37]), 4 g of 1,3-diaminopropane dihydrochloride (Wako, S Grade), and 4.5 g of anhydrous sodium acetate (Wako, S Grade) were dissolved in 100 cm^3 of EtOH and refluxed for 2 h. The obtained crude material was recrystallized from EtOH, and dark green needles of [Cu(*saltn*)] were obtained (yield: 81%; m.p.: 283–287°C).

[Cu(*salchx*)] [35, 36]: 1 g of 1,2-diaminocyclohexane (Wako, S Grade) and 4 g of salicylaldehyde (Wako, S Grade) were dissolved in 100 cm^3 of EtOH and refluxed for 2 h. The crude material was recrystallized from EtOH to afford yellow plates of *salchx*. A MeOH solution containing 3 g of copper(II) acetate (Wako) was added gradually to a MeOH solution of *salchx* (2.5 g, 200 cm^3), and dark green plates of [Cu(*salchx*)] were obtained (yield: 48%; m.p.: >286°C; found: C 61.94, H 5.26, N 7.24; calcd. for $CuC_{20}H_{20}N_2O_2$: C 62.56, H 5.25, N 7.30).

The *PVA* films were prepared by a method described earlier [32, 38, 39].

Apparatus

Electronic absorption and polarization spectra were recorded on a Shimadzu UV3101PC spectrophotometer [1]. The solid state absorption spectra were measured in KBr disks [40]. XPS were recorded on a Shimadzu ESCA-K1 X-ray photoelectron spectrometer; the binding energies were calibrated using the Au 4f level (83.8 eV). A Mac Science MXC18 X-ray diffractometer was used for the measurement of a single crystal X-ray structural analysis in which a MoK_α ray ($\lambda = 0.71073$ Å) was used as the light source. The measured diffraction data were analyzed using the SIR97 algorithm [41]. The size of the single crystal of [Cu(*saltn*)] was $0.40 \times 0.20 \times 0.15$ mm^3. Crystal data (CCDC 158311): $C_{17}H_{16}N_2O_2Cu$, $fw = 343.9$, orthorhombic, space group $Pna2_1$ (#33), $a = 12.0190(5)$, $b = 17.9710(9)$, $c = 6.8830(3)$ Å, $V = 1486.68(12)$ Å^3, $Z = 4$, $\rho_c = 1.518\ g \cdot cm^{-3}$, $F(000) = 708$, $R = 0.0504$, $R_w = 0.1208$ (298 K).

MO calculations

A threedimensionally extended PPP method, which was programmed in our laboratory for a personal computer, was used for the MO calculations [1]. In this method, the effect of the central metal ion on the π electronic systems of the ligands is considered as a point charge (+0.4 e). The two-center repulsion and resonance integrals were calculated by the *Nishimoto-Mataga* [42] and the *Nishimoto-Forster* equations [43, 44], respectively. In the configuration interaction calculations, all singly excited configurations among the highest eight occupied and the lowest eight unoccupied orbitals were taken into account. The weak interactions between almost independently existing π and π' electronic systems were considered through the resonance integrals of N–N (β_{NN}) and of O^-–O^- ($\beta_{O^-O^-}$), which were estimated by the following equation [45]:

$$\beta_{rs} = C_{rs}S_{rs}(Ip(r) + Ip(s))$$

Here, $Ip(r)$ is the ionization potential of atom r, S_{rs} is the overlap integral between atoms r and s, and C_{rs} is a constant depending on atoms r and s, *i.e.* $C_{NN} = 0.29963$ and $C_{O^-O^-} = 0.68733$.

Acknowledgements

Thanks for financial support are due to the Science Fund of the Japan Private School Promotion Foundation.

References

[1] Hoshi T, Inomaki Y, Wada M, Yamada Y (1994) Ber Bunsenges Phys Chem **98**: 585
[2] Yamada S (1999) Coord Chem Rev **190**: 537
[3] Pfeiffer P, Hesse T, Pfitznger H, Scholl W, Thielert H (1937) J Prakt Chem **149**: 217
[4] Dual C, Schlafer CW, von Zelewsky A (1979) Struct Bonding (Berlin) **36**: 129
[5] Bhadbhade MM, Srinivas D (1993) Inorg Chem **32**: 6122
[6] Dutta RL, Das BR (1988) J Scientific and Industrial Research **47**: 547
[7] Yamada S, Ohno E, Kuge Y, Takeuchi A, Yamanouchi K, Iwasaki K (1968) Coord Chem Rev **3**: 247
[8] Ohashi Y, Nakamura M (1993) Chem Lett 1389
[9] Ohashi Y, Nakamura M (1994) Bull Chem Soc Jpn **67**: 2921
[10] Ohashi Y (1997) Bull Chem Soc Jpn **70**: 1319
[11] Hall D, Waters TN (1960) J Chem Soc 2644
[12] Toy AD, Hobday MD, Boyd PD, Smith TD, Pilbrow JR (1973) J Chem Soc Dalton 1259
[13] Katsuki T (1996) J Molecular Catalysis A **113**: 87
[14] Ito YN, Katsuki T (1999) Bull Chem Soc Jpn **72**: 603
[15] Sigman MS, Jacobsen EN (1998) J Am Chem Soc **120**: 5315
[16] Samsel EG, Srinivasan K, Kochi JK (1985) J Am Chem Soc **107**: 7606
[17] Dixit PS, Srinivasan K (1998) Inorg Chem **27**: 4507
[18] Sakamoto F, Sumiya T, Fujita M, Tada T, Tan XS, Suzuki E, Okura I, Fujii Y (1998) Chem Lett 1127
[19] Singh RV, Tandon JP (1978) J Inorg Nucl Chem **40**: 2065
[20] Ferrari MB, Fava GG, Pelizzi C (1976) Acta Cryst **B32**: 901
[21] Sreenivasulu Y, Reddy KH (1994) J Indian Chem Soc **71**: 41
[22] Xiong R-G, Song B-L, Zuo J-L, You X-Z (1996) Polyhedron **15**: 903
[23] Drew MGB, Prasad RN, Sharma RP (1985) Acta Crystallogr **C41**: 1755
[24] Bernardo K, Leppard S, Robert A, Commenges G, Dahan F, Meunier B (1996) Inorg Chem **35**: 387
[25] Bullock JI, Ladd MFC, Povey DC, Tajmir-Riahi HA (1979) Acta Cryst **B35**: 2013
[26] Yamada S (1996) Coord Chem Rev **1**: 413
[27] Zerner MC, Gilda HL, Robert FK, Mueller-Westerhoff UT (1980) J Am Chem Soc **102**: 589
[28] Cory MG, Zerner MC (1991) Chem Rev **91**: 813
[29] Hasegawa M, Hoshi T (unpublished data)
[30] Dillard JG, Taylor LT (1974) Electr Spectr Relat Phenom **3**: 455
[31] Hasegawa M, Inomaki Y, Inayoshi T, Hoshi T, Kobayashi M (1997) Inorg Chim Acta **257**: 259
[32] Hoshi T, Tanizaki Y (1970) Z Phys Chem Neue Folge **71**: 230
[33] Wada M, Hasegawa M, Kobayashi M, Yoshinaga T, Hiratsuka H, Hoshi T (1999) Nippon Kagaku Kaishi 87
[34] Baba H, Suzuki S, Takemura T (1969) J Chem Phys **50**: 2078
[35] Csazar J, Balog J (1975) Acta Chim **87**: 331
[36] Funke A, Fourneau JP (1942) Bull Soc Chim Fr **9**: 806
[37] Hunter L, Marriott JA (1937) J Chem Soc 2000
[38] Hoshi T, Okubo J, Kawashima T, Iijima K, Inoue H, Sakurai T (1987) Nippon Kagaku Kaishi **1**: 1
[39] Hoshi T, Kawashima T, Okubo J, Yamamoto M, Inoue H (1986) J Chem Soc Perkin Trans 2, 1147
[40] Hasegawa M, Yamada Y, Inayoshi T, Kobayashi M, Hoshi T (1997) Nippon Kagaku Kaishi 355
[41] Altomare A, Crula MC, Camalli M, Cascarano G, Giacovazzo C, Guagliardi A, Polidori GJ (1994) Appl Cryst **27**: 435
[42] Mataga N, Nishimoto K (1958) Z Phys Chem Neue Folge **13**: 140

[43] Nishimoto K, Forster LS (1965) Theoret Chim Acta **3**: 407
[44] Nishimoto K, Forster LS (1966) Theoret Chim Acta **4**: 155
[45] Bodor N, Dewer MJS, Harget A, Haselbach EJ (1970) J Am Chem Soc **92**: 3854

Received August 21, 2001. Accepted (revised) October 20, 2001